


## Article

# Application of Graphic Statics and Strut-and-Tie Models Optimization Algorithm in Innovative Timber Structure Design

Yuanben Gao <sup>1,\*</sup>, Yiliang Shao <sup>1</sup> and Masoud Akbarzadeh <sup>2,3</sup> 

<sup>1</sup> Stuart Weitzman School of Design, University of Pennsylvania, Philadelphia, PA 19104, USA; yiliangs@alumni.upenn.edu

<sup>2</sup> Polyhedral Structures Laboratory, Stuart Weitzman School of Design, University of Pennsylvania, Philadelphia, PA 19104, USA; masouda@design.upenn.edu

<sup>3</sup> General Robotic, Automation, Sensing and Perception (GRASP) Lab, School of Engineering and Applied Science, University of Pennsylvania, Philadelphia, PA 19104, USA

\* Correspondence: yuanben@alumni.upenn.edu

**Abstract:** Timber has long been extensively employed within the construction industry as a famous, environmentally friendly, and low-carbon material. Considering that construction constitutes one of the most significant contributors to carbon emissions throughout the entire life-cycle of a building, there is an urgent desire to incorporate timber into this domain. Nevertheless, the use of timber faces inherent challenges stemming from its anisotropic nature, a result of the natural growth of timber fibers, which makes it challenging for it to function as a primary load-bearing material in coping with the various complex stresses inherent in architectural applications. Numerous designers have attempted to address this limitation through over-sized members and reinforcement at joints; however, none have satisfactorily resolved this issue in an economical manner. In this article, we introduce the Strut-and-Tie models (STM) from Graphic Statics (GS) and a topological optimization algorithm. This algorithm has the capability to generate a ‘load-minimizing path’ STM based on external load support conditions and the maximum structural path span. Regardless of the complexity of the initial external loads, each load transfer path in the optimized STM bears loads in only one direction, representing an optimal solution with minimal internal loads that align seamlessly with the characteristics of timber. Consequently, we endeavor to adopt this optimization algorithm to propose a structural design methodology, with the aspiration of designing structural systems that harness the unique attributes of timber perfectly and applying them to various architectural scenarios. Ultimately, we conclude that structural systems designed based on optimized STM are adaptable to diverse architectural contexts, and when applied to small-scale buildings, this method can save approximately 20% of material consumption compared to conventional timber frame structures, while in the case of mid-rise to high-rise buildings, it can lead to a material savings of approximately 5%.

**Keywords:** graphic statics; timber; strut-and-tie models; structure optimization



**Citation:** Gao, Y.; Shao, Y.; Akbarzadeh, M. Application of Graphic Statics and Strut-and-Tie Models Optimization Algorithm in Innovative Timber Structure Design. *Buildings* **2023**, *13*, 2946. <https://doi.org/10.3390/buildings13122946>

Academic Editor: Francisco López-Almansa

Received: 22 October 2023

Revised: 20 November 2023

Accepted: 22 November 2023

Published: 25 November 2023



**Copyright:** © 2023 by the authors. Licensee MDPI, Basel, Switzerland. This article is an open access article distributed under the terms and conditions of the Creative Commons Attribution (CC BY) license (<https://creativecommons.org/licenses/by/4.0/>).

## 1. Introduction

### 1.1. Current Status and Limitations of Timber Structural Buildings

Timber as a building material has been highly regarded across various industries due to its structural rigidity and environmental sustainability, making it a common presence in the realm of sustainable construction materials [1]. However, when examining numerous existing buildings, it is evident that timber is predominantly used as decorative panels. For instance, residential buildings utilize timber for flooring due to its environmental sustainability and cost-effectiveness [2], while concert halls opt for timber in ceiling and wall finishes due to its high porosity [3]. In the domain of interior design, designers can fully exploit the potential attributes of timber, such as its porosity, eco-friendliness, lightweight nature, and flexibility, to meet diverse needs.

In utilizing timber as a structural support material, numerous constraints have been imposed on its application. While wood has demonstrated favorable characteristics in terms of carbon emissions and life-cycle assessments, its utilization as the primary load-bearing structure for large-scale high-rise construction projects has encountered limitations. Despite the commendable performance of wood, particularly in smaller-scale timber residential structures and certain urban artistic installations, many substantial, high-rise architectural endeavors still opt for steel and concrete structures to serve as the primary load-bearing framework. The adoption of wood as a predominant structural element in extensive architectural projects is subject to several constraints and challenges [4–6]. Timber is a natural material characterized by significant anisotropic properties due to the nearly circular annual growth rings, which are approximately perpendicular to the direction of timber grain growth. The performance of timber varies drastically depending on whether the load is applied along the longitudinal (fiber) direction. When subjected to longitudinal loads (in the direction of fibers), timber exhibits compressive strength comparable to that of concrete. However, it is prone to bending and fracturing when facing shear and transverse stresses [7–9]. Therefore, special treatments are required for timber to serve as a load-bearing material in multi-directional stress scenarios in mid-rise to high-rise buildings. Common approaches currently employed include: (a) Structural strapping and reinforcement, involving the use of larger timber components than standard ones, along with the use of steel components to bind and secure the structural elements [10]. While this method increases the load-bearing capacity of structural components, it also escalates construction costs. (b) Embedding dried hardtimber inserts into notches or slots milled on the top surface of timber elements, causing them to form curves. These inserts expand as they adjust to the moisture content (MC) and climate of the surrounding timber, creating pre-stress forces [11]. This approach compromises the mechanical performance of timber components from the outset. (c) Precision cutting of timber components into specific units and assembling them in the form of arches or stable systems (mechanical force equilibrium) to ensure that they can bear loads effectively [12]. This method is only suitable for certain specific timber structural scenarios. (d) Precise cutting technology facilitated by robots can accurately assess the compressive performance of each section of timber and subsequently reassemble them into a mutually beneficial structural configuration to ensure cost-effectiveness and structural rigidity [13]. However, this method is not conducive to widespread application, as each structural component requires customized evaluation. (e) There is a considerable body of research aiming to utilize lignin extraction for the secondary processing of wood, thereby enhancing the compressive and tensile strength of wood fibers and upgrading the chemical composition of wood into a more advanced material [14]. However, this secondary processing not only adds to the overall cost but also transforms the nature of wood fundamentally, especially after impregnation with polyurethane composite materials. Consequently, the wood essentially becomes a different material, losing its inherent environmental sustainability. In essence, these methods do not directly address the limitations of timber's anisotropy while fully utilizing it, instead relying on increased economic costs to enhance structural mechanical properties.

In this study, we aspire to design an innovative structural form that can fully exploit the anisotropic characteristics of timber. On one hand, we avoid additional chemical treatments of timber to ensure its cost-effectiveness and sustainability. Simultaneously, we seek to ensure that individual timber structural components only need to bear stress in one direction, thereby maximizing the performance given their anisotropic properties. Furthermore, we aim to create a novel timber structural system in which timber can theoretically adapt to various stress conditions. We only need to choose the most suitable combination of timber components based on different stress requirements. This way, we effectively utilize the timber structure's mechanical performance and anisotropy.

### 1.2. Graphic Statics and the Ground Truss Optimization

Graphic Statics (GS) is a method used to analyze the equilibrium of forces and moments in static structures through the application of geometric techniques. It operates based on the principles of resolving and combining forces, similar to the principles of the parallelogram of forces [15–17]. Developed in the 19th century, GS was introduced to analyze and design truss systems and compression-only arches. It offers a visual and intuitive approach to comprehending the distribution of forces within a structure, simplifying the process of designing and optimizing structural systems. This method enables us to accurately analyze the internal forces within a structure when subjected to external loads by constructing the Force Diagram.

GS finds applications across various fields of mechanical analysis. It can be employed for analyzing the impact of moving vehicle loads on bridge structures using influence line analysis [18], assessing the stress distribution in complex industrial machinery components [19], and performing performance analysis in maritime engineering, among others. In the realm of structural analysis in construction, Strut-and-Tie Models (STM) are models established for reinforced concrete structures using GS [20,21]. Through STMs, one can precisely determine which parts of a reinforced concrete structure experience compression in the concrete and tension in the steel when subjected to various stresses. Therefore, STMs not only serve as analysis models but also have the potential to guide structural design. However, while Graphic Statics provides explicit control over STM geometry and internal force magnitudes within the same state of global or external equilibrium, it can only offer a binary assessment of the feasibility of the structure [22,23]. In situations involving more complex continuous systems (e.g., truss, cantilevered structure), Graphic Statics can confirm the feasibility of internal force transmission while maintaining external force balance, meaning that as long as an STM can be established, the structure is theoretically feasible. However, theoretical feasibility is not a mechanism for evaluating the rationality of a structure. It is theoretically feasible for all crazy cantilever and extreme large-span structures to achieve external equilibrium conditions and establish STM through Graphic Statics analysis, but they inevitably differ from each other. Therefore, in addition to achieving balance and establishing STM through Graphic Statics analysis, a filtering method must also be employed to guide structural design.

To address this issue, Mozaffari et al. [24] developed an optimized load path algorithm for Strut-and-Tie Models using topological optimization and finite element analysis methods, combined with the principles of Graphic Statics [24]. This method is distinct from others that use finite element analysis, such as BESO (Bidirectional Evolutionary Structural Optimization), which treats density as a variable to search for the optimal material distribution [25]. STM optimization, on the other hand, focuses on optimizing load paths and leverages the advantages of LAYOPT (Layout Optimization refers to the process of systematically arranging or organizing elements within a given space to achieve specific objectives or criteria) and Graphic Statics to bridge the gap between the two, resulting in a load-minimizing path. This approach engages Graphic Statics in the automatic process of generating STM solutions and their Force Diagrams without the need to predefine the Form Diagram. The implementation incorporates equations from LAYOPT [26], principles of reciprocal diagrams [16], and the algebraic formulation of Graphic Statics [27]. The implementations of LAYOPT and Automatic Graphic Statics (AGS), as well as the Minkowski Sum [28] operation, are integrated into a single computational setup to generate a valid truss model, its Force Diagram, and constant stress fields [24]. By setting initial external equilibrium conditions, which primarily include external loads and support conditions, along with specifying the maximum path for internal force transmission allowed by the STM, the algorithm outputs a load-minimizing path within this maximum allowable range (presented as a Force and Form Diagram). This “load-minimizing path” refers to the most economical path for internal force transmission within the specified input conditions. This path indicates the core structural elements and provides design recommendations for reinforcing steel elements in reinforced concrete structures.

Initially, the purpose of this code was to analyze STMs in concrete structures and provide recommendations, mainly focusing on algorithmic analysis. In this paper, we aim to apply the STM generated by this optimization algorithm, which yields one-way load-bearing paths in timber structures. Each path in the optimized algorithm-generated STM is designed to accommodate the mechanical properties and anisotropy of the timber material perfectly. Additionally, this algorithm can generate STMs tailored to different external equilibrium conditions, allowing us to use different sizes of timber to meet these requirements. If we can materialize the load-minimizing path to generate the structural prototype, this structure should represent the most economical solution while ensuring mechanical performance. This will be discussed further in subsequent sections of this paper.

### *1.3. Research Gap and Objectives*

In this experiment, we address the challenge within contemporary timber structural design, where the full potential of wood material anisotropy is not fully realized in an economically and environmentally sustainable manner. Our aim is to introduce the optimized Stress Transfer Matrix (STM) algorithm into our novel timber structural design. In this innovative timber structural system, each timber member is designed to resist stress loads in a single direction, thereby maximizing the utilization of wood material anisotropy. Simultaneously, the optimized STM algorithm allows for precise calculation of the load-bearing capacity of each structural member. Consequently, this novel timber structural system enables accurate assessment of the dimensions of each member based on load-bearing requirements, thereby minimizing excess material consumption and significantly enhancing the economic and environmental sustainability of timber structures. In summary, we envision that our newly designed timber structure, while successfully meeting the adaptability criteria of a structural system, will use fewer structural materials than conventional timber structures, thereby improving overall material efficiency.

## **2. Materials and Methods**

In this methodology, a total of four steps are required to achieve the final optimized design of timber structures with STM (Strut-and-Tie Models), as illustrated in Figure 1 above. Step 1 involves volume segmentation, where the building is divided into smaller units according to specific rules and hierarchies. These units consist of floor slabs and supporting structures. The purpose of this step is to collect basic building load information for subsequent structural generation. Step 2 involves operations on structural units, where the potential STM support surfaces within each unit are separated, and load information is further applied to each STM support surface to determine whether the STM is in external equilibrium. This step also collects information for the optimization algorithm. Step 3 is the optimization algorithm, where external load information required for each STM is input into the optimization code, resulting in the Form Diagram and Force Diagram of the load-minimizing path for each STM. Step 4 involves importing the information from the Form and Force diagrams into our Grasshopper and Python tools to generate a materialized truss structure. Finally, these elements, along with floor slabs and curtain walls, are assembled to create a complete building structure model. After the model is generated, it is essential to conduct a comparative analysis of the experimental results. On one hand, this analysis aims to verify whether the novel timber structural system is capable of addressing various scenarios. On the other hand, a comparative analysis of structural material consumption is conducted to validate its economic potential.



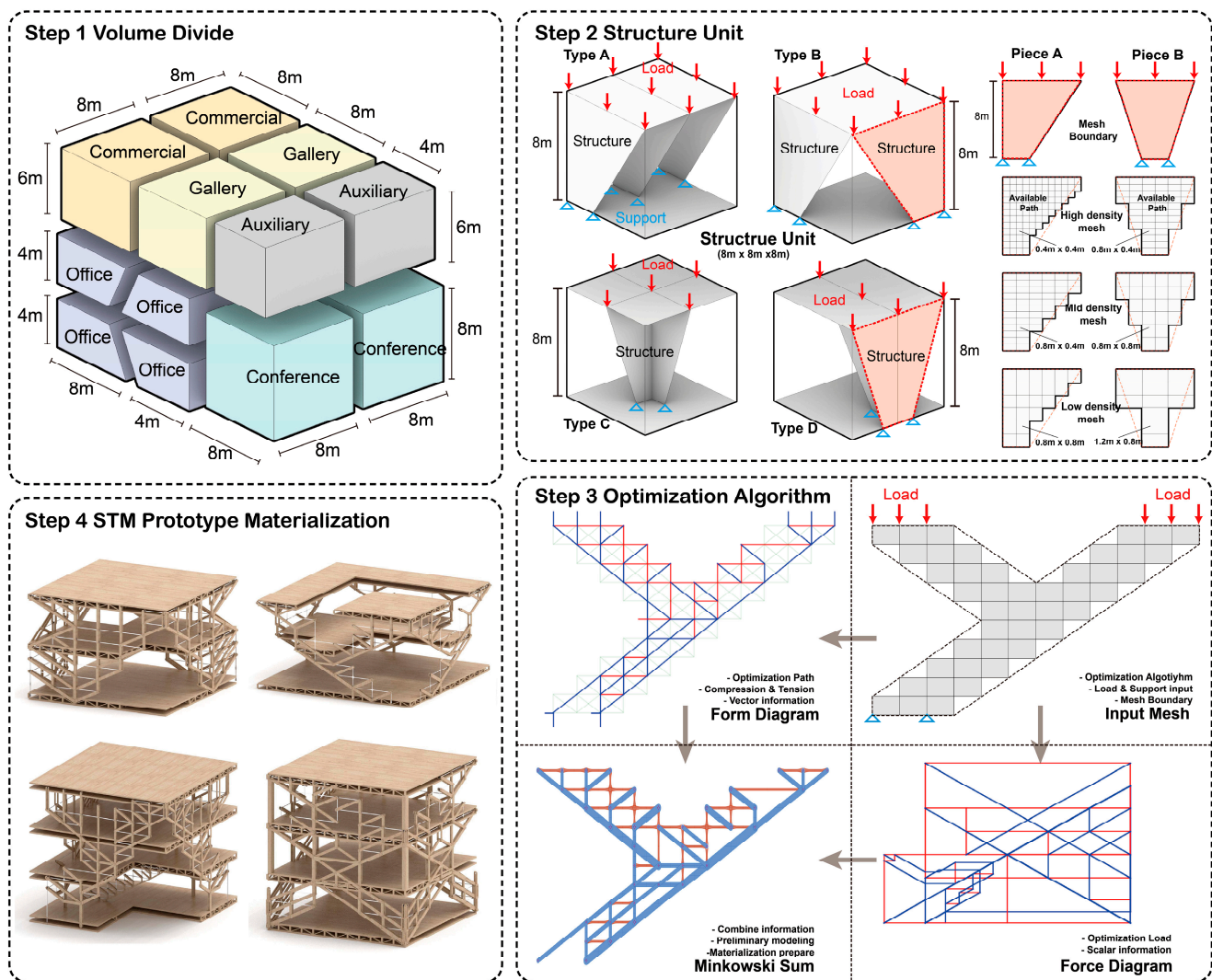


**Figure 1.** Methodology.

### 2.1. Volume Segmentation

To segment any given building volume and collect background information, the following hierarchical steps and size requirements need to be followed. The purpose is to provide all external information and structural layout constraints for subsequent STM structure generation and optimization.

- (1) **Building Level:** Initially, the main dimensions of the building, such as plan dimensions and building height, are determined based on specific requirements, including upper-level planning, floor area ratio, site conditions, and more. This tool is not suitable for designing structures with irregular shapes, such as curved or non-standard forms.
- (2) **Layer Level:** Layer level in this context refers to the different levels of a building, particularly the classification of building floors. After the architectural form is determined, it becomes necessary to categorize the floors based on the functions they support, such as office areas, equipment rooms, non-occupiable areas, and so on. Different functional categories impose distinct standard load values on the structure. We collect information on permanent and variable loads from Eurocode 1 [29], enabling the deduction of the load requirements for each section of the floor area. This specific load information is then imported into the Grasshopper plugin of Rhino 7 for subsequent form-cutting procedures. Through these steps, a shaded volumetric

diagram is generated, encompassing the building's outer outline and load information for all floor functionalities.

- (3) Unit Level: This stage involves the design of structural units. The objective is to divide a large building into numerous smaller units, each with a height of 1–2 floors. These units may have different sizes, but they must adhere to the following principles:
  - (i) The unit's base must be a solid floor slab and not suspended in empty space.
  - (ii) The vertical faces of the unit must have at least two solid faces (a single solid face cannot support a floor slab).
  - (iii) The plan dimensions of the unit should be around 8 m × 8 m.
  - (iv) Units should avoid spanning multiple floor function zones.
  - (v) Unit shapes should be regular, such as rectangular or terraced shapes, avoiding curved or irregular surfaces.

Finally, for this set of split units, they are imported into Grasshopper and assigned coordinates based on their positions in 3D space to facilitate subsequent operations on individual units.

## 2.2. Structural Units

Before conducting the algorithmic optimization, it is necessary to translate the external equilibrium information for each unit into input data that the algorithm can recognize. This requires a separate segmentation operation for each unit, focusing on transferring the unit and its load information to each structural support surface and translating them into load vectors, structural grids, and other geometric information. The aim is to provide all the required external input information for the subsequent STM optimization algorithm.

First, the unit is exploded into different faces, distinguishing between solid structural faces (those allowed to participate in load transfer) and other dividing faces (those not bearing structural loads, such as partitions, walls, and decorative surfaces). Subsequently, for each solid face, Grasshopper delineates a control line defining the maximum range of structural elements. The intersections of the control line and the bottom plate are automatically designated as available support points. Note that before dividing the solid faces, it is essential to ensure that all solid faces can support the loads of the upper floor slabs and transmit them through the support points on the bottom plate. Next, we need to summarize and enter load-related information, including load application points, load directions, load magnitudes, and potential support point positions. In this step, we calculate the load values to be borne by each structural face based on the layout of the supporting floor slabs. This information helps determine where the loads will act on the structural faces. At this point, we have gathered all the external information for each structural face (load application points, load directions, load magnitudes, and available support points).

Finally, based on the information from key points (load points and support points), Grasshopper selects an appropriate modulus to control the density of the grid that covers the entire outline of the structural face. Grasshopper defaults to filling the entire outline with equally sized grid units, but manual adjustments can be made if special customization is needed. Note that the grid must ensure a connection between every load application point and any support point. Thus, we obtain the distribution of the internal structure grid.

## 2.3. STM Optimization

In this step, we need to utilize the STM Optimization Algorithm to input the external equilibrium information obtained in the previous step and follow the following steps to generate an STM with the load-minimizing path. The code will output Force and Form diagrams containing all the internal load information for this STM (Figure 2).

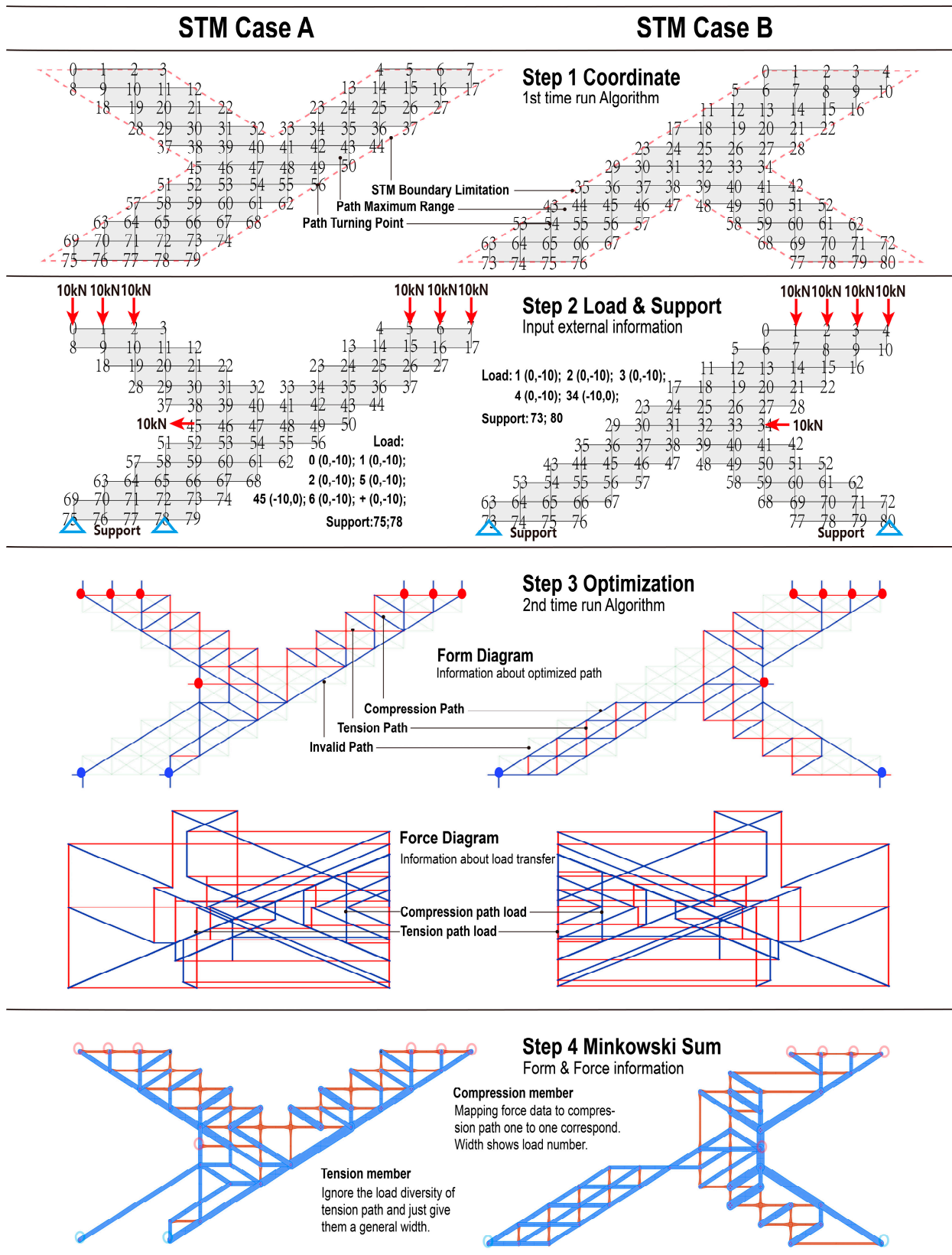


Figure 2. Optimization STM.

Step 1: Define Initial Grid Point Coordinates. In this step, we need to import the initial structural grid into the algorithm to assign coordinates to each point in the initial grid.

Step 2: Input Load and Support Information. Based on the coordinate numbering, we input all the loads for this structural face into the code. For example, “Point 6 (0, −10)” represents a load of 10 kN acting downward along the  $y$ -axis at point 6. After inputting all the loads, we enter the coordinates of the support points in the “support” section of the code.

Step 3: Generate Optimized STM Diagram. Using the input information mentioned above, we run the code once more, which will generate an STM structure with the “load-minimizing path.” The output includes Form and Force Diagrams. The Form Diagram represents the optimized structural form, with blue lines indicating compression paths and red lines indicating tension paths. The Force Diagram graphically depicts the forces in each path, with the length of each edge indicating the magnitude of the force. Each edge in the Force Diagram corresponds to a path in the Form Diagram, and they are mutually perpendicular. The combination of these two diagrams results in the Minkowski sum diagram, which contains all the information required for this STM structure.

Step 4: Iteration and Superposition. Due to the effect of gravity, the loads from upper structural units eventually transfer to the supports of lower units. Therefore, we need to consider these additional loads as part of the input data in a process similar to iteration and superposition. Ultimately, all the loads will be transferred to the supports at the bottom of the building. It is essential to repeat the above steps multiple times to ensure that all the floor loads of the building are optimized layer by layer through the STM. This results in a series of Optimized STMs.

Note: During the algorithm’s generation process, errors may occur due to an unreasonable distribution of loads and support points. Additionally, the optimized STM may have an irregular shape. This indicates that the initial external environmental information was not in equilibrium (e.g., an overhanging structure cannot achieve balance with only one support point). In such cases, adjustments to the external equilibrium of the units are necessary.

#### 2.4. STM Materialization Prototype

In this phase, we extract information from the previously optimized Force and Form Diagrams, transforming it into an actual STM (Strut-and-Tie Model) steel and timber hybrid truss structure. This STM is converted into a steel and timber truss prototype that can be used for practical production using Rhino.

- (a) Steel cables as tension members: Timber is an excellent material for compression members (due to its anisotropy), but it has limited tensile strength. Steel, on the other hand, is suitable for tension members and is lightweight, making it ideal for our structure.
- (b) Timber as compression members: In large-scale buildings, the structure itself can become a significant load. To improve structural efficiency, we plan to calculate the dimensions of each timber structural member based on the required load capacity. Since these timber members only need to function as compression members, we refer to Eurocode 5 [30] for controlling parameters regarding timber column design.

Axial load capacity refers to the maximum axial (or longitudinal) compressive load that a timber column can withstand without causing failure. This capacity represents the maximum safe load that the column can bear when subjected to compression. See Equation (1)

$$N = A \times F_c \quad (1)$$

where  $N$  is the axial load capacity.  $A$  is the cross-sectional area of the column.  $F_c$  is the characteristic axial compressive strength of the timber.

Critical buckling load refers to the load at which a structural member (such as a column or strut) becomes unstable and buckles under the applied compressive force. Buckling is a



mode of structural failure where the member undergoes lateral deflection or deformation, often leading to catastrophic failure. See Equation (2)

$$P_{critical} = \frac{\pi^2 \times E \times I}{K^2 \times L^2} \quad (2)$$

where  $P_{critical}$  is the critical buckling load.  $E$  is the modulus of elasticity of the timber.  $I$  is the second moment of area of the column section.  $K$  is the effective length factor (code-dependent).  $L$  is the second moment of area of the section.

Section modulus is a geometric property of a structural cross-section that quantifies its resistance to bending. It is a fundamental parameter used in structural engineering, particularly in the analysis and design of beams and other structural members subjected to bending loads. See Equation (3)

$$S = \frac{d^2 \times b}{6} \quad (3)$$

where  $S$  is the section modulus,  $d$  is the width of the section, and  $b$  is the depth of the section.

Bending strength is a material property that measures a material's ability to withstand bending or flexural loads without breaking or permanently deforming. See Equation (4)

$$M_r = \frac{f_{c0,k} \times S}{\gamma_M} \quad (4)$$

where  $M_r$  is bending strength.  $f_{c0,k}$  is the characteristic axial compressive strength of the timber.  $S$  is the section modulus.  $\gamma_M$  is the material safety factor.

Deflection refers to the degree to which a structural element or component deforms or displaces under an applied load. It represents the bending or sagging of a structural member when subjected to external forces, such as loads or moments. See Equation (5)

$$\delta = \frac{5 \times w \times L^4}{384 \times E \times I} \quad (5)$$

where  $w$  is the distributed load.  $L$  is the length of the material.  $E$  is the elastic modulus of the material.  $I$  is the second moment of area of the section.

After the calculations mentioned above, we can determine the required cross-sectional dimensions for each individual structural member to meet the load requirements.

- (c) Modular Production: We will modularize the timber members based on their load capacities. In other words, each structural member within the STM (Strut-and-Tie Model) will have no more than six different cross-sectional sizes (many similar timber structural members are grouped into the same size category for ease of production). Steel components, being lightweight, will be uniformly arranged according to the maximum tension dimension (Figure 3—Preliminary Modeling).
- (d) Double-Layer CLT Members: To enhance the stability of the STM structure itself, we will symmetrically arrange CLT (Cross-Laminated Timber) members [31]. This arrangement consists of a specific number of CLT panels of a given size on both the left and right sides, with a steel cable in the middle (Figure 3—Correct Position). These components will be welded together at specific angles using rivets (the angles are determined by the shape of the initial grid).

Figure 3 illustrates the actual process of generating the STM Materialization prototype in Rhino, with the following key steps:

- (1) Input and Matching Data: We use Python and Grasshopper tools to input and group the data from the Optimized STM [32]. This involves establishing the initial positions of the members based on the one-to-one mapping between the Force and Form Diagrams (Figure 3—Input Diagram and Matching Data).



- (2) Preliminary Modeling: Cross-sectional dimensions are mapped onto the Form Diagram to generate actual timber members, which are then repositioned to match the corresponding locations on the Form Diagram (Figure 3—Preliminary Modeling).
- (3) Correct Position: After generating and mapping all the members, they are symmetrically arranged at each node to ensure that the members do not overlap and no gaps or voids are left (Figure 3—Correct Position).
- (4) Generate Spacer and Bolts: Details such as spacer elements and bolts for steel components at the bottom support are generated (Figure 3—Generate Spacer and Bolts).

Note: To prevent certain lightweight timber members from becoming too slender and fragile, we have predefined a minimum member length-to-thickness ratio in the code to ensure structural feasibility.

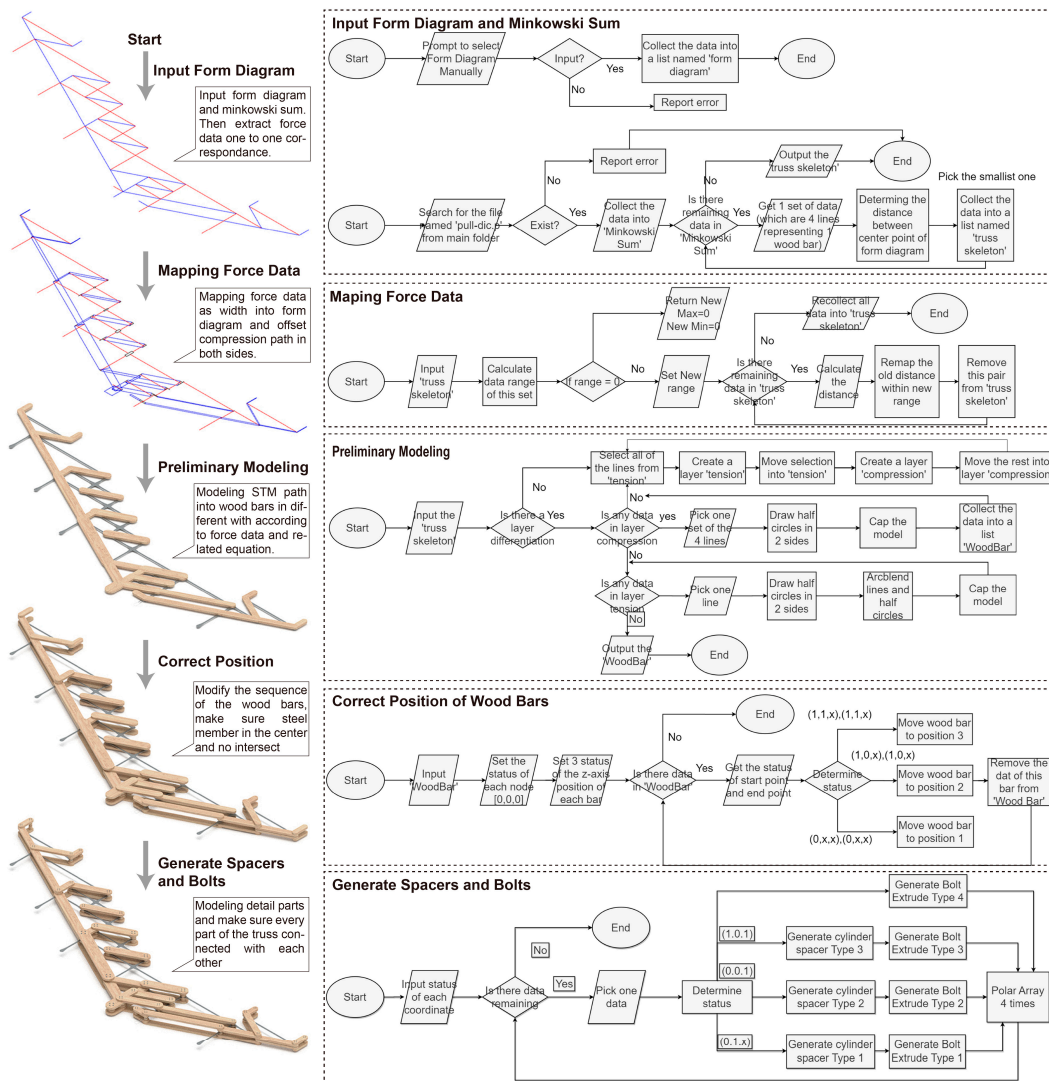


Figure 3. Materialization.

## 2.5. Data Analysis

### 2.5.1. Optimized STM

Since each optimized STM is already an optimized path, we need some metrics to quantitatively reflect the internal load transmission and distribution within each STM to enable a horizontal comparison of their effectiveness.

The Load-Minimizing Path obtained after code optimization refers to the optimal solution under given input conditions (load information, mesh boundary). However,

different load values and STM boundary constraints will yield different optimal solutions. We need to find an appropriate method and metrics to quantify and analyze these optimal solutions. The load values for each path within the Load-Minimizing Path are determined based on input load values. Therefore, a direct comparison of path load values does not make sense. Instead, we need metrics that reflect the relationships between all path load values within any Load-Minimizing Path and their magnitudes relative to the input load values. This is similar to analyzing the distribution and variability of load values, akin to statistical load value distribution and dispersion measures [33,34]. Therefore, we employ the calculation of the standard deviation (see Equation (6)) for discrete random variables to analyze the data within the Force Diagram and Form Diagram [35,36].

$$\sigma = \sqrt{\frac{1}{N} \sum_{i=1}^N (x_i - \frac{1}{N} \sum_{i=1}^N x_i)^2} \quad (6)$$

- (1) Average Load Standard Deviation (see Equation (7)): We calculate the moment (path length  $\times$  path load) for each path and use these values in the standard deviation formula mentioned above. This average load standard deviation reflects the dispersion of path moments within the STM. A larger value indicates a higher degree of dispersion, meaning that a significant portion of the load is concentrated in a few paths. Conversely, a smaller value suggests that the load is evenly distributed among the paths.

$$\gamma = \sqrt{\frac{1}{N} \sum_{i=1}^N (L_i \times F_i)^2 - (L \times F)^2} \quad (7)$$

where  $L = \frac{1}{N} \sum_{i=1}^N L_i$ ,  $F = \frac{1}{N} \sum_{i=1}^N F_i$ ,  $N$  represents the total number of paths in the STM,  $L_i$  represents the length of each path, and  $F_i$  represents the load value corresponding to each path in the STM.

- (2) Excess Load Standard Deviation (see Equation (8)): To further analyze the dispersion of load values for paths with loads greater than or equal to the initial load values, we employ a statistical approach that combines the interquartile range (reflecting the first and third quartiles) and standard deviation calculations from robust statistics [37,38]. We filter and collect the load values of paths that have loads greater than or equal to the initial load values using Grasshopper and then perform standard deviation analysis. We replace the average load with the initial load values during this calculation. This method provides a standard deviation calculation that reflects the dispersion of load values for all paths with loads greater than the initial load values.

$$\delta = \sqrt{\frac{1}{N} \sum_{j=1}^{N_j} (L_j \times F_j)^2 - (L \times f)^2} \quad (8)$$

where  $L = \frac{1}{N} \sum_{i=1}^N L_i$ ,  $N$  represents the total number of paths in the STM, and  $N_j$  represents the total number of paths in the STM with internal loads greater than the initial input load.  $L_j$  represents the length of each path, and  $F_j$  represents the load value corresponding to each path in the STM.

The parameter  $\gamma$  reflects the uniformity of load transfer within the STM, while  $\delta$  reflects the efficiency of load transfer within the STM. Since vector loads undergo load value changes whenever there is a change in the path direction, it is common for many paths to have load values greater than the initial load values. As the load values on paths increase, it requires better mechanical performance of the components to support them. This can increase the burden on structural materials, so a smaller  $\delta$  indicates higher efficiency in the use of structural materials.

### 2.5.2. Analysis of the STM Materialization Prototype

In Section 3.4, we transform the optimized STM into a specific steel–timber hybrid truss through materialization. In the subsequent Section 3.2, we assemble these steel–timber hybrid trusses into different architectural chunks and calculate the timber material consumption. We also collect data on timber material consumption for existing timber structures and compare the two sets of data for analysis.

## 3. Results

In this chapter, we have established numerous sets of design experiments and conducted analyses and summaries of the experimental results. It is primarily divided into two parts: the first part consists of four sets of experiments (Section 3.1) aimed at the lateral comparison of optimized STMs. By modifying parameters in different instances of the optimized STM of the same type, we compare the results to determine external factors that can influence the internal load equilibrium and structural efficiency of the STM. The second part comprises two sets of experiments (Section 3.2) where the materialized STM steel–wood hybrid truss is applied in different architectural scenarios. One objective is to demonstrate the adaptability of this truss to various architectural contexts, while another is to analyze and summarize the wood material consumption for each chunk of the truss, considering the variations in application scenarios.

### 3.1. Factors Influencing the Performance Variation of Optimized STM

#### 3.1.1. Group 1: Long-Distance Cantilevered STM

**Experimental Description:** The objective of this set of experiments is to compare the standard deviation metrics of different long-span cantilever structures' STMs, evaluating their respective advantages and influencing factors. Figure 4 illustrates a set of experimental configurations for long-span cantilever structures, with the input mesh featuring large-span cantilever structures as prototypes. The support points and load points are significantly distant in both horizontal and vertical dimensions. These STM configurations allow for a substantial release of the space below without affecting the net height of the underlying building. They are suitable for large-span spaces or double-height spaces, offering versatility in architectural applications.

**Experimental Result:** As shown in Chart 1 (the data in the table represent the two types of standard deviations mentioned earlier, which are analytical values reflecting the degree of dispersion in a set of data; hence, they are dimensionless), the trends of the average load standard deviation and excess load standard deviation for the six STMs are almost identical. The only difference between the two standard deviation calculations lies in whether to exclude paths with load values less than the initial values. When combined with their Force Diagrams and Minkowski sums, it is evident that almost all path loads exceed the initial load values, and the excess load values are substantial. Comparing the values of each STM horizontally, we find that STM 1D has the best performance in terms of both indicators. Observing the input meshes of 1B, 1C, 1D, and 1E, it can be seen that they only differ in mesh subdivision. We analyze that STM 1D's aspect ratio of mesh cells performs better with vertical loads. When horizontal members are longer, significant changes in the direction angle occur when vertical loads are transmitted along the paths, resulting in higher vector load values. STM 1F introduces a load on the opposite side compared to STM 1A but significantly reduces the load standard deviation and excess load proportion. Preliminary analysis suggests that symmetrical stress on both sides creates a better external balance environment, which greatly influences the internal load transmission optimization of STM. Therefore, for initial meshes with identical boundaries, selecting the appropriate mesh subdivision type based on the external load environment can significantly impact the efficiency of optimized STM. The balance environment created by the initial input load points and support points itself has a considerable influence on the optimal load paths within the STM.

**Experiment Contributions:**

- (1) This experiment demonstrates that the configuration of different initial external environments influences the form and efficiency of the final optimal load paths.
- (2) The efficiency of various optimal load paths varies, and the most suitable initial external environment gives rise to the most efficient optimal load path.

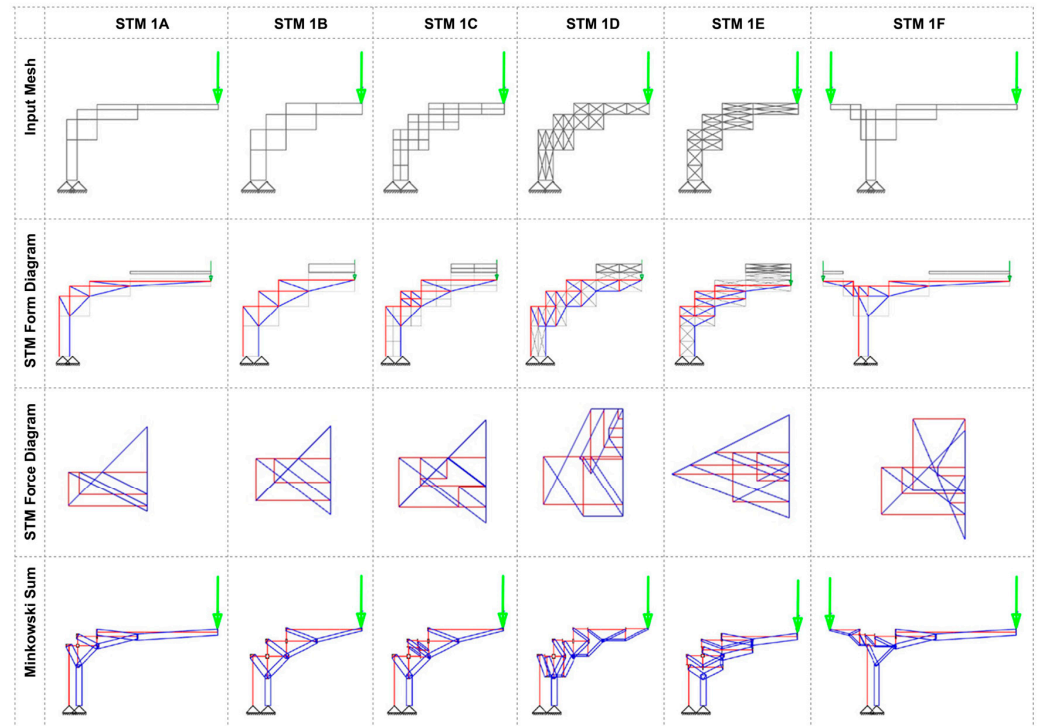


**Figure 4.** STM Group 1. Explanation: The input mesh in the first row represents the input information for the optimized algorithm. The mesh signifies paths for the transfer of loads. Green arrows indicate the position and direction of the loads, while the bottom triangles represent the location of supports. The form diagram in the second row represents the optimized STM. Blue denotes compressed paths, and red denotes tension paths. The force diagram in the third row includes information about load magnitudes, where each red or blue edge corresponds to the load magnitude of the corresponding red or blue path in the form diagram. The Minkowski sum in the fourth row is the optimized STM model with load information, generated by combining the two sets of information in a one-to-one correspondence.

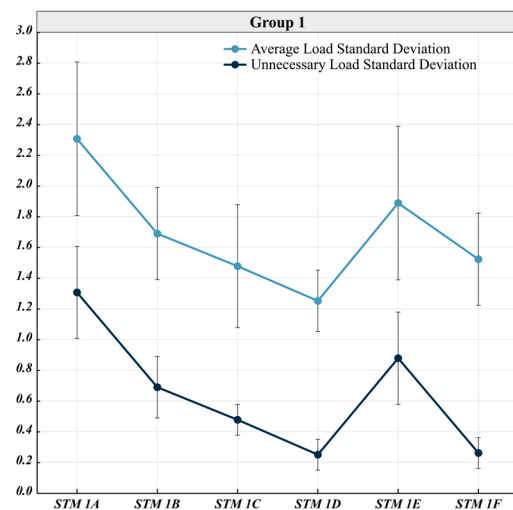


**Chart 1.** Standard Deviation of Group 1.

### 3.1.2. Group 2: Mid-Distance Cantilevered STM

**Experimental Description:** This set of experiments shown in Figure 5 focuses on the comparative analysis of mid-range cantilever STMs, aiming to further validate the conclusions drawn in Group 1 and explore additional findings. The input mesh for this group also features cantilever structures, but with a more moderate cantilever distance compared to the previous set, providing complementary analysis to the results obtained in the previous group. Additionally, a more in-depth analysis is conducted to explore the impact of multiple load points versus a single load point on the final optimized STM. This analysis will determine the advantages and disadvantages of different connection methods between floor loads and supporting structures.

**Experimental Result:** Observing the line trends in Chart 2, we notice that, except for STM 2C, the trends for the two standard deviations remain consistent for the other STM. Preliminary analysis suggests that STM 2C, with multiple load points on one side, did not alter the external environment of the cantilever significantly, hence not improving load uniformity. However, it reduced the number of concentrated load paths, thereby enhancing overall efficiency. We then compare the two standard deviations of STM 2B, 2D, and 2E to further validate the conclusions regarding appropriate mesh subdivision from Group 1. Finally, the comparison between STM 2F and STM 2B reflects the impact of the external balance state on the STM.

**Experiment Contributions:**

- (1) Selecting an appropriate mesh subdivision method based on different external load environments (load position, quantity, and direction) contributes to improving the balance and efficiency of the STM model.
- (2) Reasonable distribution and arrangement of all external loads (symmetrical arrangement, uniform distribution, etc.) aid in generating a better external equilibrium environment, thereby influencing the optimization of STM generation.

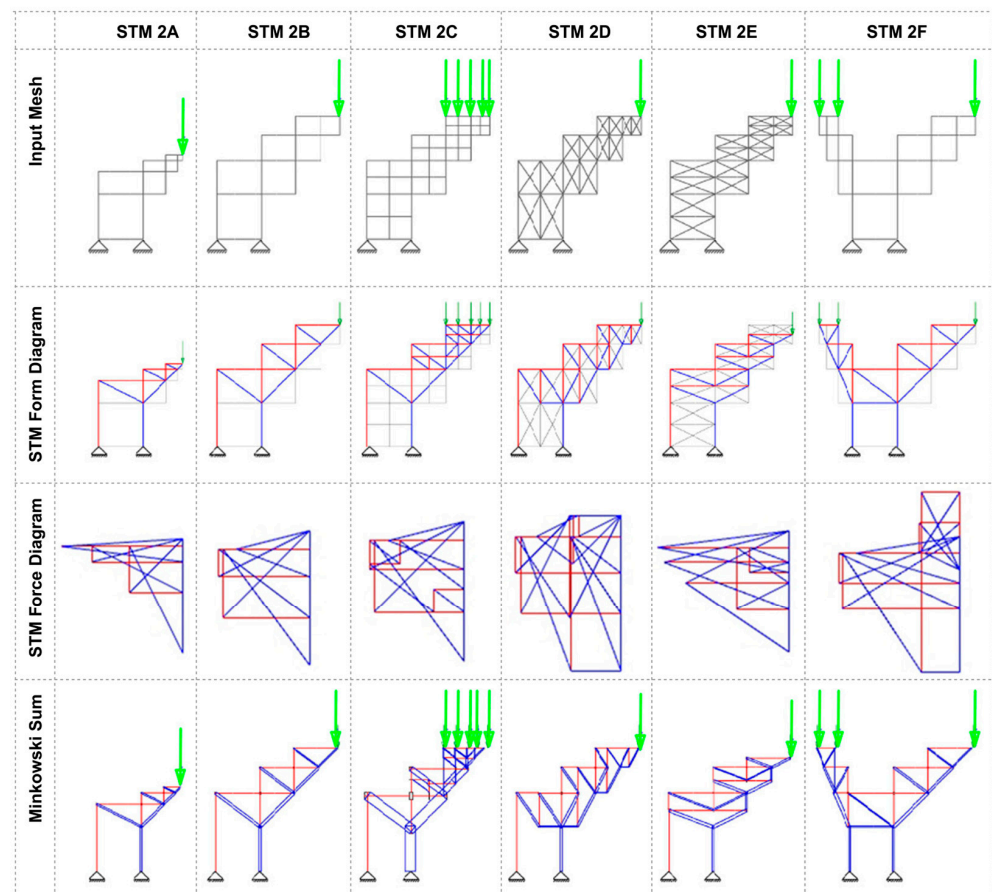
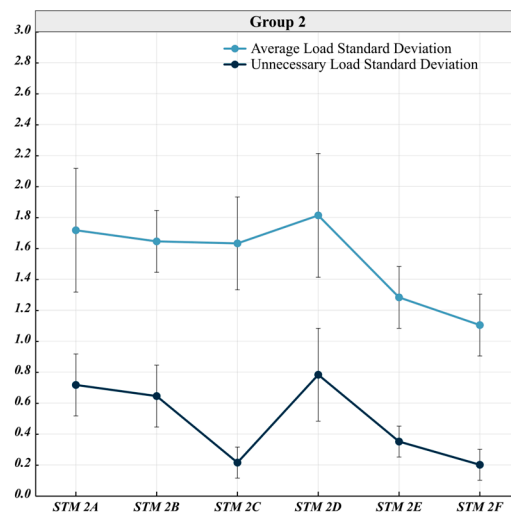


Figure 5. STM Group 2.





**Chart 2.** Standard Deviation of Group 2.

### 3.1.3. Group 3: Symmetrical STM 1

**Experimental Description:** In this set of experiments, we aim to explore how adjusting the edges and internal divisions of the initial mesh will affect the overall STM while keeping the external balance environment unchanged. We seek to understand how local modifications to the mesh boundaries, while maintaining the support and load information and the initial mesh density, can impact various mechanical properties of the STM. The purpose of this experiment is to address common structural conflicts with other disciplines in architectural design, such as the need for MEP (mechanical, electrical, and plumbing) systems to pass through the structure or architectural constraints on structural boundaries (Figure 6).

**Experimental Result:** Chart 3 reveals that the average load standard deviation and excess load standard deviation for all STMs in this group are smaller compared to the previous two groups. This is due to the well-established initial external balance environment, which confirms the previous conclusions. Observing the overall trends in the lines, we can see that the trends for both types of standard deviations are roughly synchronized but not entirely identical, indicating a certain relationship between the balance and efficiency values of the STM. Furthermore, STM 3D, which represents an STM with no limitations on the initial mesh, has the lowest average load standard deviation and excess load standard deviation. This suggests that any restriction on the minimum load path can impact the performance of the STM. On the other hand, the other STMs have slightly higher values for load transmission standard deviation and excess load proportion due to limitations on the optimal path. However, STM 3F exhibits only a slightly higher value than STM 3D in load transmission standard deviation and excess load proportion, which can be considered negligible. It also provides an open space in the middle that can accommodate MEP systems or even a small number of people. Therefore, it is preliminary to conclude that the influence of different paths within each minimum load path STM on the overall performance of the structure may vary.

**Experiment Contributions:** In situations where the initial external environments are essentially similar, the imposition of local restrictions on load transfer paths has an efficiency impact on the final generation of the minimal load path.

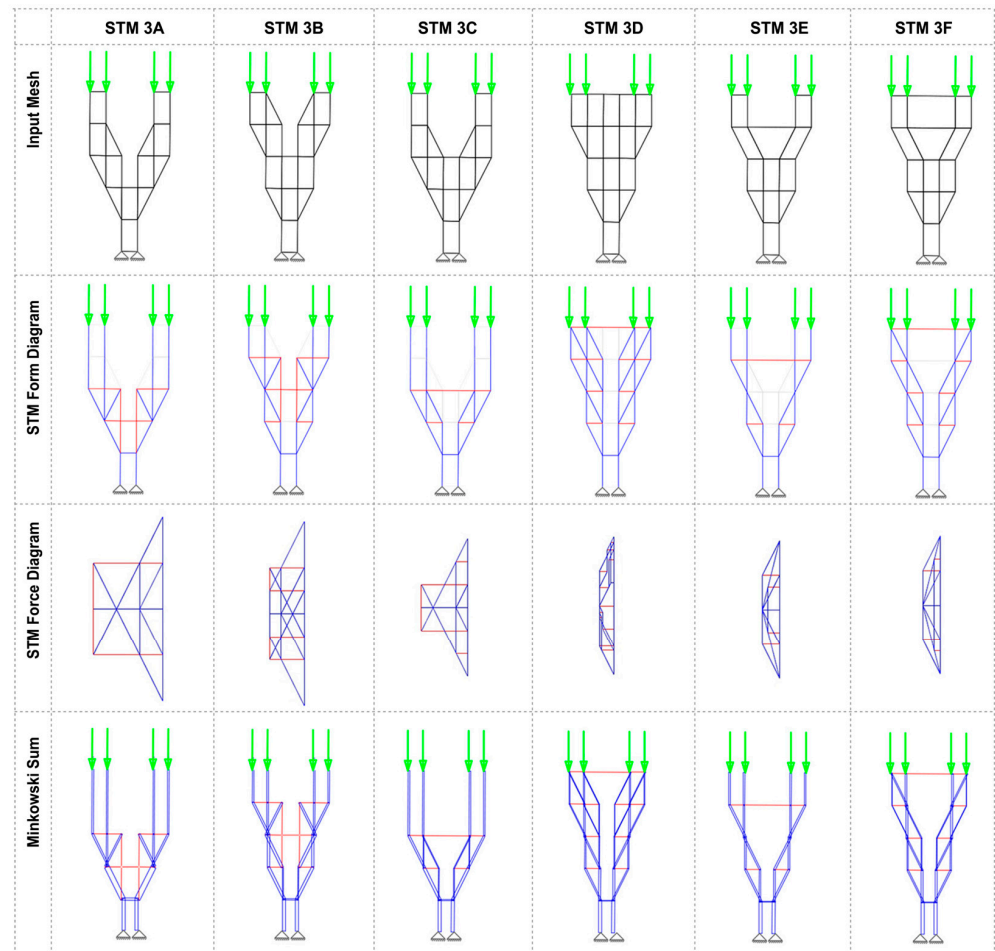


Figure 6. STM Group 3.

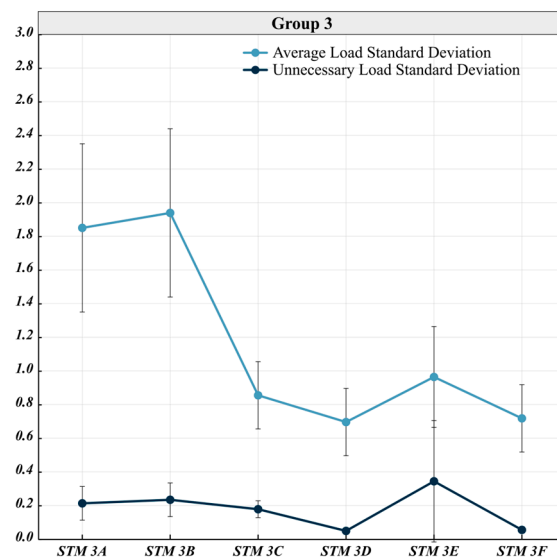


Chart 3. Standard Deviation of Group 3.

### 3.1.4. Group 4: Symmetrical STM 2

Experimental Description: In this group of experiments shown in Figure 7, we further investigate the conclusion from Group 3 that different paths have varying degrees of influence. Similar to Group 3, this group explores the impact of adjusting the initial mesh

on the final optimal path. However, in this group, we use smaller mesh subdivisions to increase the number of paths, further substantiating the previous reasoning.

**Experimental Result:** Chart 4 shows that STM 4D has the smallest standard deviation, once again confirming the significance of the minimum load path. STM 4F exhibits performance that is second only to the optimal path. Preliminary analysis indicates that the uppermost tensile path in the minimum load path is crucial, while the absence of the vertical mesh path in the middle has little overall impact. Routing all loads through the two edge paths still ensures efficiency. Therefore, STM 4F can release the central area for other purposes without compromising overall performance.

**Experiment Contributions:** Even within the context of the minimal load path, there are variations in the influence between paths. Therefore, under the condition of identifying and preserving the critical path within the optimal route, locally altering the secondary internal structure of the initial mesh allows for the partitioning of specific regions for other functionalities while ensuring structural performance.

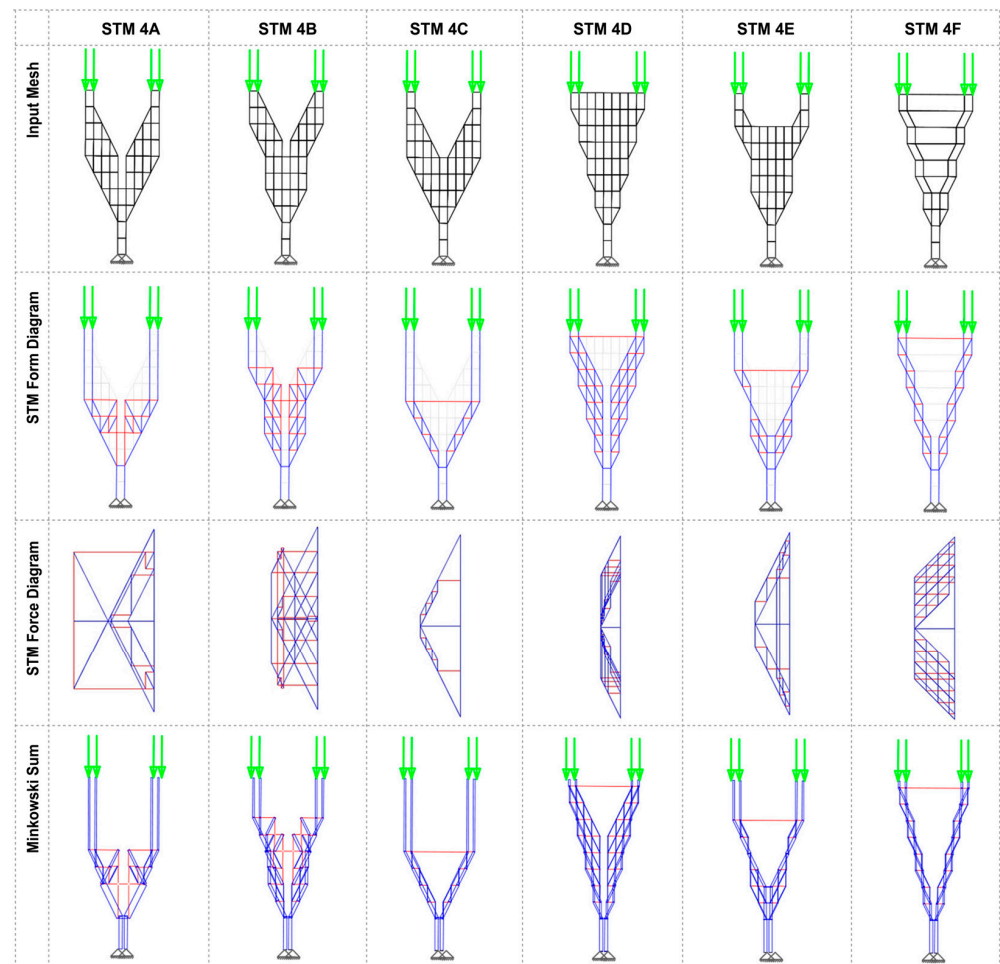
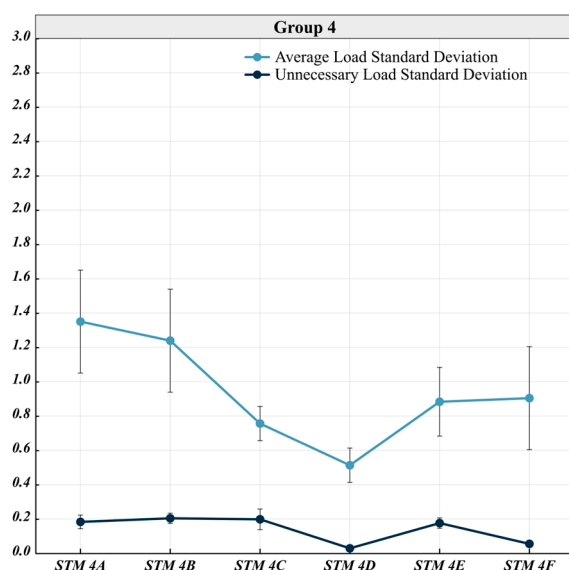


Figure 7. STM Group 4.



**Chart 4.** Standard Deviation of Group 4.

### 3.2. Materialization Truss Consumable Analysis

#### 3.2.1. Stairs

In this group of experiments, we aim to compare the consumables of structure STMs used in various forms of stairs and determine whether this optimized STM can be applied to various stair variations. Different STM-generated trusses were used for different stair scenarios: straight-run stairs, switchback stairs, evacuation stairs, and landscape stairs, among others.

By combining Figure 8 with Table 1, we can observe the differences in trend size between Stair 2 and Stair 1, resulting in Stair 2 having a longer STM length, a greater overhang, and a higher structural burden, leading to more STM consumables. Stair 4, in comparison to Stair 2, adds an intermediate flight of stairs, resulting in different trend distributions and changes in STM form, but STM consumables are smaller than those of Stair 2. Stairs 5–6 form a control group where the only difference is the position of the intermediate landing. Using a Y-shaped STM allows for direction changes in multi-flight stairs. The results indicate that the STM consumables for both Stair 5 and Stair 6 are similar, suggesting that changes in the vertical position of the intermediate landing do not significantly burden the structure. Stair 7 is designed with symmetrically arranged bidirectional stairs, consuming approximately 50% more structural material compared to Stair 1. However, the width of the bidirectional stairs increases by 100% (Table 1). Therefore, symmetric arrangement is a viable approach. Thus, we conclude that steel–timber composite trusses generated using STM can be applied to various stair scenarios.

**Experiment Contributions:** The steel–wood hybrid truss generated using the STM has the potential to be applied in various complex scenarios of staircases. This optimization algorithm has the capability to generate customized and economically optimal staircase support structures based on different factors such as staircase angles, requirements, spans, and other considerations.

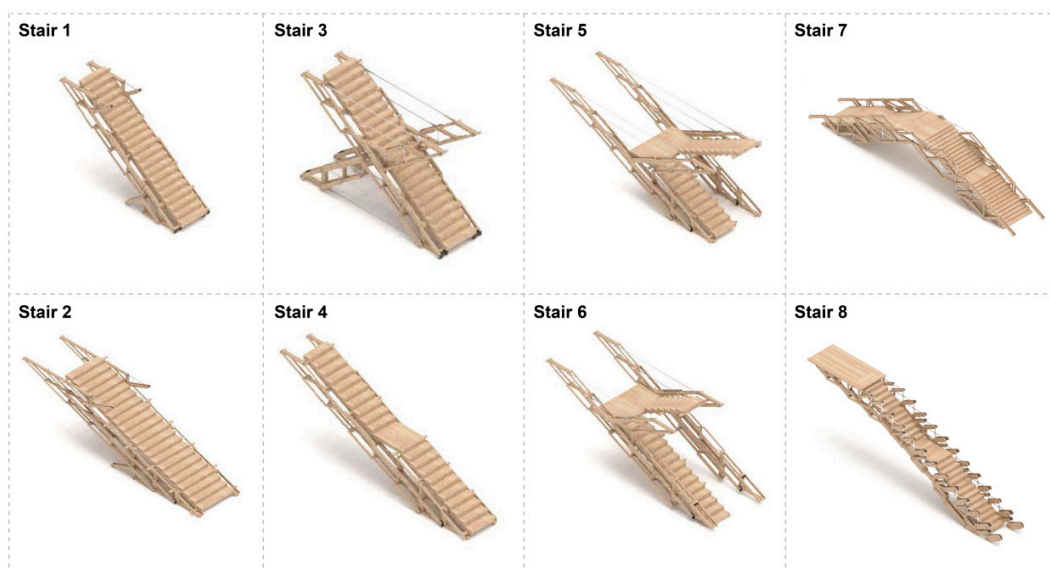


Figure 8. Stair Group (Render from Rhino 7).

Table 1. Stair Group Information.

| Stair No. | Tread Size (mm) | Tread Distribution | Stair Overall Load (kN) | STM Height (m) | STM Length (m) | STM Timber Consumable (m <sup>3</sup> ) |
|-----------|-----------------|--------------------|-------------------------|----------------|----------------|---|
| 1         | 250             | 22                 | 164.8                   | 3.4            | 5.7            | 0.7296                                  |
| 2         | 350             | 22                 | 208.2                   | 3.4            | 8.2            | 1.0048                                  |
| 3         | 250             | 22                 | 167.1                   | 3.4            | 5.7            | 1.7184                                  |
| 4         | 350             | 11 + 11            | 181.9                   | 3.4            | 8.2            | 0.9792                                  |
| 5         | 250             | 11 + 11            | 189.2                   | 3.4            | 8.9            | 1.1904                                  |
| 6         | 250             | 14 + 8             | 152.6                   | 2.8            | 6.9            | 1.1712                                  |
| 7         | 250             | 11 + 11            | 326.6                   | 3.4            | 11.5           | 1.3920                                  |
| 8         | 250             | 22                 | 128.1                   | 3.4            | 8.2            | 1.5264                                  |

### 3.2.2. Small Chunk Group

In this set of experiments, we attempted to apply the steel–timber composite trusses generated by this optimized STM to small two- to three-story building chunks and analyzed structural consumables and various spatial attributes. We calculated the effective building area and timber structural material consumption for each chunk to assess the practicality and economic feasibility of applying the optimized STM to small-volume buildings.

As shown in Figure 9 and Table 2, both Chunk 1 and Chunk 2 are two-story buildings. Although different types of STM were used, the average structural consumables per unit area are similar (as seen in the consumables per unit area column). Similarly, Chunk 3 and Chunk 4 are both three-story chunks, and their average structural consumables are also close. However, when comparing Chunks 1 and 2, as well as Chunks 3 and 4, it is evident that as the building area supported by the chunk increases, the consumables per unit area value increase. Smaller supported building areas result in higher structural efficiency. Therefore, it is initially concluded that this optimized STM seems to have an advantage in saving material for small building volumes: increasing the number of stories and building area both lead to an increase in structural consumables per unit area.



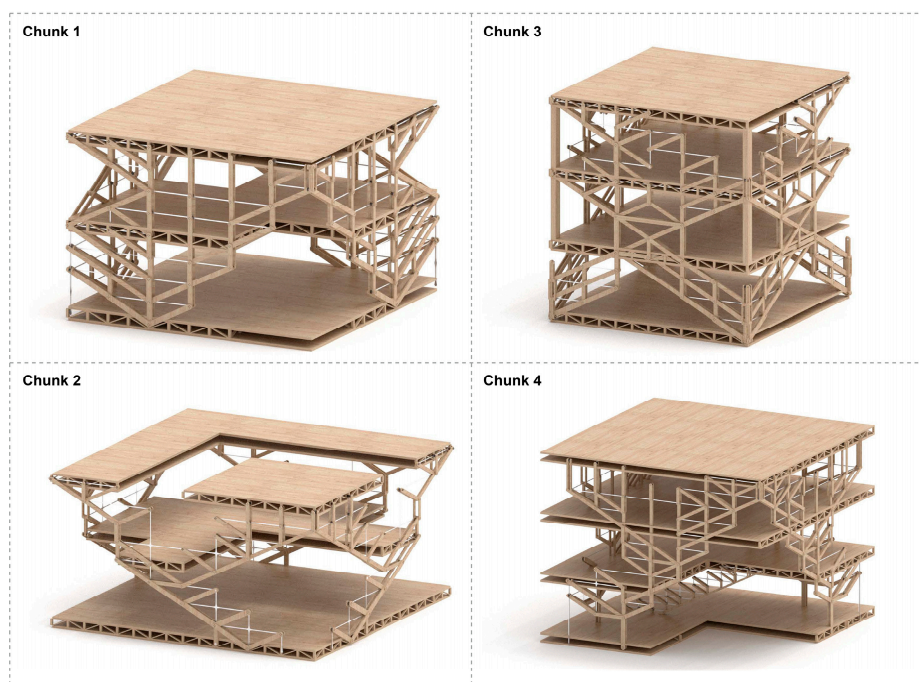


Figure 9. Small Chunk (Render from Rhino 7).

Table 2. Small Chunk Information.

| Chunk No. | Standard Plan (m) | Chunk Height | Floor Area (m <sup>2</sup> ) | Chunk Overall Load (kN) | STM ILSD | STM ULR | STM Timber Consumable (m <sup>3</sup> ) | Consumable per Unit Area (m) |
|-----------|-------------------|--------------|------------------------------|-------------------------|----------|---------|---|------------------------------|
| 1         | 12 × 12           | 8            | 258                          | 32,250                  | 1.09     | 0.25    | 26.8062                                 | 0.1039                       |
| 2         | 16 × 16           | 8            | 244                          | 30,500                  | 2.19     | 0.81    | 24.4245                                 | 0.0983                       |
| 3         | 12 × 12           | 8            | 432                          | 54,000                  | 1.68     | 0.49    | 50.2848                                 | 0.1134                       |
| 4         | 16 × 16           | 16           | 562                          | 70,250                  | 1.36     | 0.31    | 63.9556                                 | 0.1108                       |

Experiment Contributions: This set of experiments demonstrates that the novel steel–wood hybrid truss can serve as a primary support for small-scale constructions. While the overall material consumption may vary slightly depending on the type of truss, it generally remains consistent at a comparable level for the overall structure.

### 3.2.3. Large Chunk Group

In this set of experiments, we compared and analyzed the structural consumables of high-rise buildings supported by steel–timber composite trusses generated by various optimized STM. All STM chunks had a floor height of 3.8 m, and standard floor areas were around 600 m<sup>2</sup>. The key differences are as follows: Chunks 1 and 2 have larger floor areas with more double-height spaces, while Chunks 3 and 4 primarily consist of single-level spaces with some special areas. Additionally, Chunks 1, 2, and 3 used two different scales of STM (the density of lower-level STM mesh units was half that of upper-level STMs) to avoid excessive density in the lower members. In contrast, Chunk 4 used the same scale of mesh units to avoid overly thick lower-level members.

As shown in Figure 10 and Table 3, Chunks 1 and 2 have similar visual effects, and the ‘consumables per unit area’ values are very close. It is initially concluded that the choice of STM form for chunks primarily results in visual differences, similar to the conclusion drawn from the previous set of small chunks. Truss type does not significantly impact structural material efficiency. Chunks 3 and 4, due to their use of uniformly sized mesh units, result in higher densities in the lower optimized STM trusses, leading to an increase in the number of members but avoiding excessively thick structural members. However, in

terms of numerical values, Chunks 3 and 4 have higher consumables per unit area values than Chunks 1 and 2. In summary, applying the optimized STM to medium to high-rise buildings results in a reduction in structural material efficiency. Although there is a slight advantage, it is not as significant as observed in the previous set applied to small two- to three-story buildings.

**Table 3.** Large Chunk Information.

| Chunk No. | Standard Plan (m) | Chunk Height | Level Number | Floor Area (m <sup>2</sup> ) | Chunk Overall Load (kN) | STM Timber Consumable (m <sup>3</sup> ) | Consumable per Unit Area (m) |
|-----------|-------------------|--------------|--------------|------------------------------|-------------------------|---|------------------------------|
| 1         | 40 × 16           | 35           | 10           | 4850                         | 606,250                 | 573.755                                 | 0.1143                       |
| 2         | 40 × 16           | 35           | 10           | 5120                         | 641,440                 | 613.376                                 | 0.1168                       |
| 3         | 36 × 18           | 35           | 10           | 6280                         | 785,060                 | 807.608                                 | 0.1284                       |
| 4         | 36 × 18           | 35           | 10           | 5650                         | 706,250                 | 692.691                                 | 0.1228                       |

**Experiment Contributions:** In terms of construction materials, the steel–wood hybrid truss generated through the topological optimization algorithm of STMs exhibits a greater economic advantage when applied to small-scale constructions. When applied to mid- to high-rise buildings, the average material consumption may increase due to the increased height of the building. However, the overall structural material consumption per unit area generally remains at a consistent level.

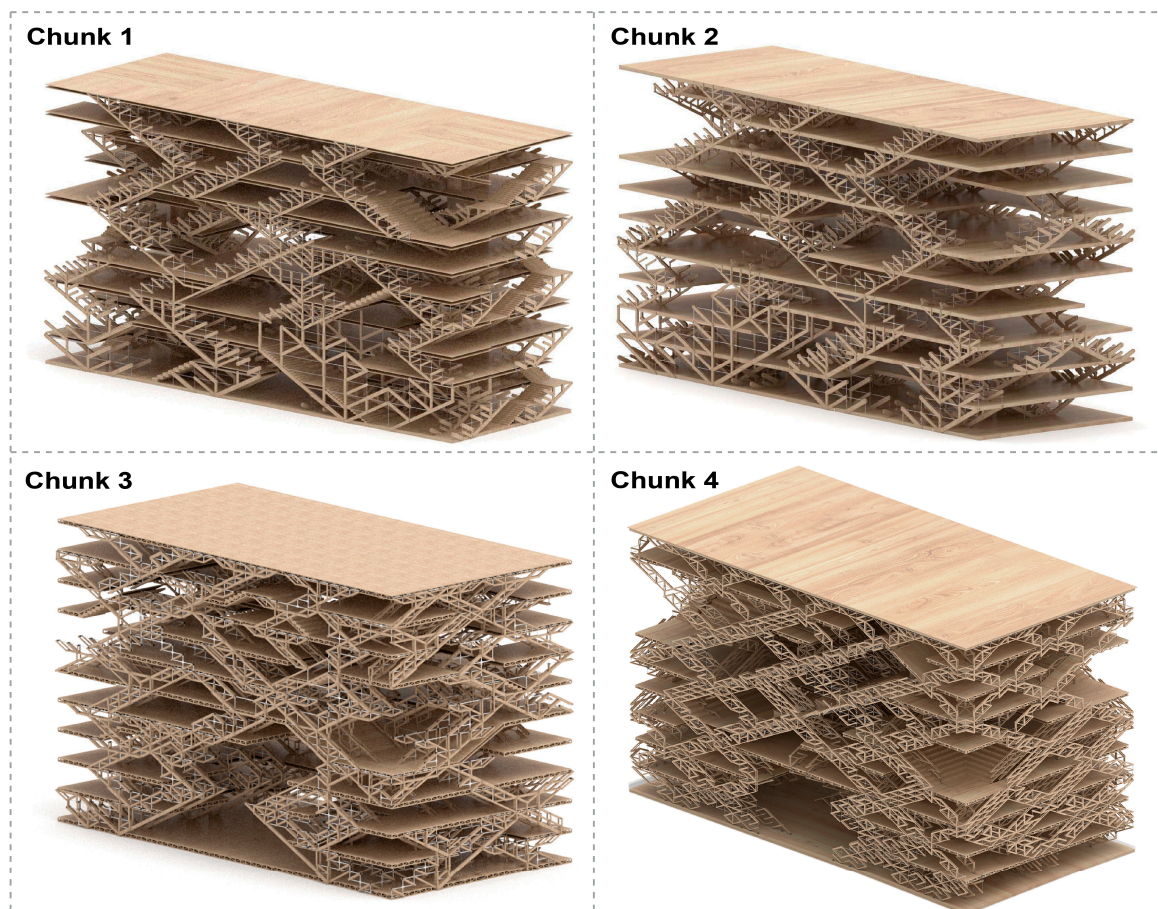


**Figure 10.** Large Chunk (Render from Rhino 7).

### 3.3. Summary of Experimental Results

Based on the comparative analysis of the various experiment results, we conclude the following:

- (1) The novel timber structural system exhibits strong adaptability, capable of generating different types of optimized timber structures according to different initial external environments. It can be applied in various scenarios, including staircases, small-scale buildings, high-rise constructions, and more.
- (2) The average overall structural material consumption of the novel timber structure remains consistent, regardless of the truss style used. The efficiency of structural material consumption shows only minor variations.
- (3) The efficiency of structural material consumption is higher, and economic benefits are greater when the novel timber structure is applied to small-scale constructions.

### 3.4. Threats to Experimental Validity and Mitigation Measures

The above experiments are limited to static load analysis in building structures, meaning that the analysis and calculations of dynamic loads generated by activities such as human movement or wind loads are inaccurate in this experiment. The algorithm used in this experiment can only compute the optimal load path for a single state, and dynamic loads were approximated by converting them into static maximum load values distributed evenly across all load points. However, this simplification may not accurately represent real-world scenarios, where concentrated activities of people or strong unidirectional winds can result in concentrated and fluctuating loads on specific load points over time.

To address this limitation and enhance the algorithm, future optimizations could involve incorporating dynamic load values using a more scientific computational approach in the calculation of the overall optimal load path. For random events like crowd activities, it is suggested to introduce different transformation parameters based on the frequency of such events. This would allow the conversion of dynamic loads into loads with varying weighting factors (not a simple average) to be included in the algorithmic calculations. This approach would make the overall simulation more representative of real-world conditions.

## 4. Discussion

### 4.1. Comparison with Other Timber Structures

To validate whether the optimized STM truss structures can enhance the cost-effectiveness of timber structures, we need to compare the structural consumables of the chunks from Section 3.2 with other timber structures. As we can see in Table 4, we selected House Charlie [39] and Building Arbo [40] as comparison objects, both of which are standard timber frame buildings. Calculating the dimensions of the timber structural beams and columns as well as the building areas from the data in the respective references, we found that the consumables per unit area for House Charlie is 0.1306, and for Building Arbo, it is 0.1224.

Comparing these values with the analysis of the eight chunks from Section 3.2, it becomes evident that the optimized STM truss structures contribute to reducing structural material consumption and improving the cost-effectiveness of timber structures. For small to medium-sized chunks, an average saving of 15–20% in structural material consumption is achieved, while for high-rise building chunks the average saving is around 5–10%. This reaffirms that the application of optimized STM truss structures is more advantageous for small to medium-sized buildings.

In addition, we have conducted a comparative analysis of our structural material consumption with two other wood structure optimization measures mentioned earlier: structural strapping and reinforcement [10] and robotic precision cutting [13]. From the data in the table, it is evident that when applied to small-scale building volumes, our novel optimized structure exhibits significantly lower average structural material consumption and higher economic benefits. In the case of large-scale high-rise building volumes, the average material consumption of the other two methods is slightly lower than that of our novel timber structural system. However, considering the construction of large-scale



high-rise buildings using structural strapping and reinforcement and robotic precision cutting methods, the former relies heavily on numerous concrete materials, and the latter incurs substantial costs related to robotic operations. Therefore, we conclude that our novel timber structure still possesses a pronounced economic advantage.

**Table 4.** Comparison with other timber buildings (consumables per unit area).

| House Charlie | Building Arbo | Structural Strapping and Reinforcement | Robotic Precision Cutting | Our Study (Small Chunk) | Our Study (Large Chunk) |
|---------------|---------------|--|---------------------------|-------------------------|-------------------------|
| 0.1306        | 0.1224        | 0.1183                                 | 0.1091                    | 0.0983–0.1134           | 0.1143–0.1284           |

#### 4.2. Prefabrication and Structural Metabolism

The initial purpose of using the optimized STM algorithm to generate steel–timber hybrid structures was to find the most economical way to leverage the anisotropic properties of timber. Besides reducing structural material consumption, we also considered that timber has a shorter lifespan compared to concrete and steel structures. Therefore, construction waste and future replacements are also important economic considerations. The STM-optimized trusses effectively break down a large timber structure into numerous smaller pieces that are easy to quantitatively produce and assemble. Combining these pieces with prefabricated construction methods not only reduces carbon emissions on the construction site but also facilitates the replacement of structural components in the future (Figure 11).

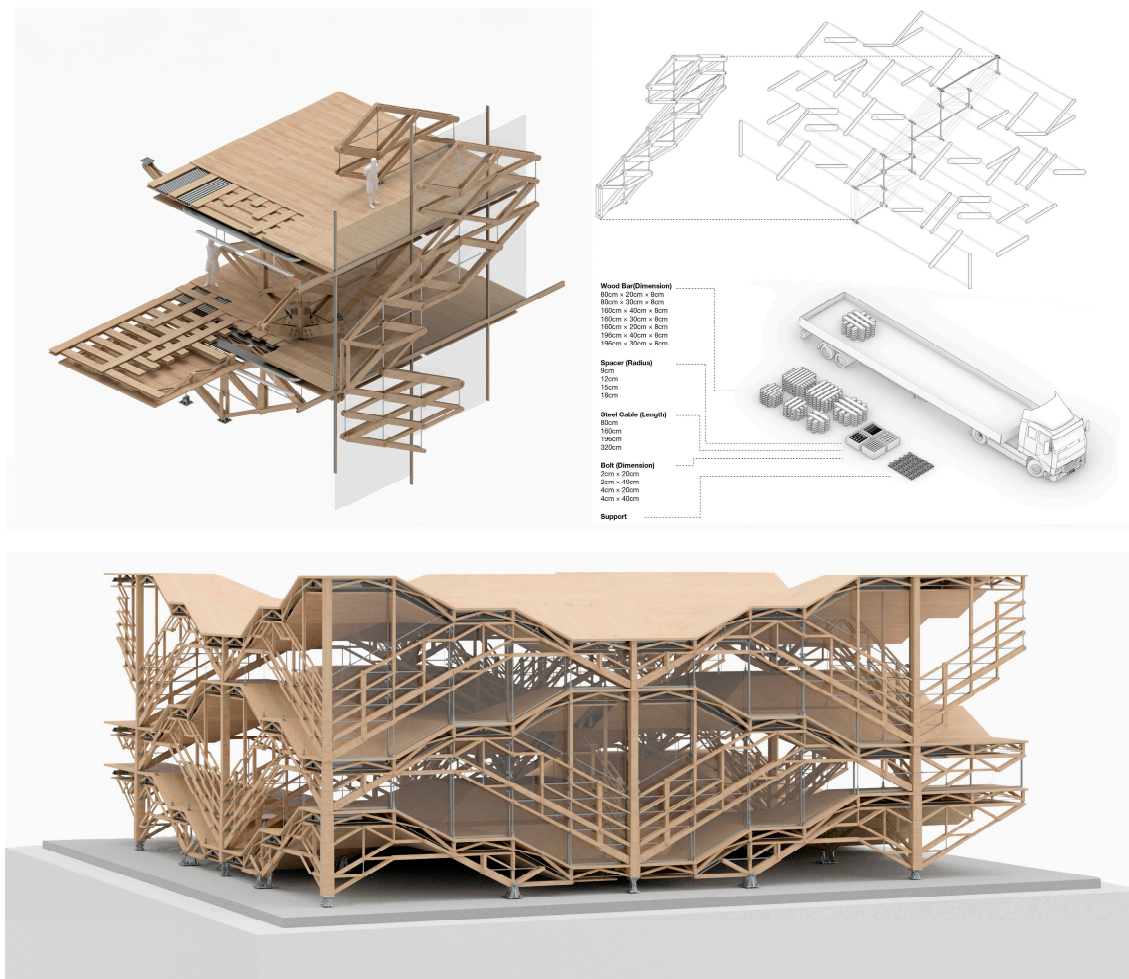


**Figure 11.** Prefabrication and construction detail (Render from Rhino 7).

In practical construction scenarios, we recommend the following approach:

**Site Survey and Preparation:** Start with site survey and preparation, including excavation work and the installation or preparation of building-related utilities, in accordance with local regulations. The on-site assembly process should only begin after the completion of underground work and the first-floor slab.

**Prefabrication and Delivery:** Collaborate with timber manufacturers to prepare fixed-size and quantity CLT pieces, along with all necessary steel cables and components required for construction. These should be delivered to the construction site.

**Sequential Assembly:** Refer to the assembly steps outlined in Sections 3.1 and 3.2. Assemble the units from the bottom to the top. Complete the assembly of lower structural units before moving on to the upper ones.

**Stability Checks:** During assembly, first assemble individual structural STMs. Once an STM is completed, erect two to three structural STMs together and perform vertical stability tests. Ensure structural stability and strength before attaching the floor plates and trusses that belong to that unit. Install elements like glass curtain walls and interior building components after the building's civil construction part is completed.

By combining STM-optimized trusses with prefabricated construction methods, you can achieve not only cost-effectiveness but also greater sustainability and flexibility in the construction process, which is crucial for addressing both construction waste and future structural component replacement.

#### *4.3. Limitations of the Study and Proposed Solutions*

##### *4.3.1. Limitations of Graphic Statics*

Graphic Statics, while a powerful and intuitive method for analyzing structures, has certain limitations. Here are some of the limitations associated with Graphic Statics. **Applicability to Statically Determinate Structures:** Graphic Statics is primarily applicable to statically determinate structures, meaning structures where the equilibrium conditions can be completely satisfied using only statics equations. For statically indeterminate structures, additional methods, such as the flexibility or stiffness method, are typically required. **Limited to Two Dimensions:** Graphic Statics is most commonly applied in two-dimensional problems. While it is possible to extend graphical techniques to three-dimensional problems, the complexity increases significantly, and alternative methods may be more practical for 3D analysis. **Sensitivity to Initial Assumptions:** The graphical approach in Graphic Statics relies on a set of assumptions and idealizations. Deviations from these assumptions, such as changes in geometry or support conditions, can affect the accuracy of the results.

##### *4.3.2. Diversity in Wood Types*

It is essential to acknowledge that many of the simulated experiments conducted in this study did not fully incorporate the actual diversity and complexity of wood types. Various factors, such as the type of wood, its origin, and age, significantly influence wood properties. Different types of wood, such as pine, birch, oak, and spruce, exhibit distinct characteristics in terms of compressive strength, durability, and other performance indicators. In this study, we primarily focused on the most common Cross-Laminated Timber (CLT) for computational purposes.

To address this limitation, future research can delve into a more comprehensive exploration of wood material varieties suitable for this innovative timber structural form. Specifically, conducting simulated studies on truss structures using different wood types may provide valuable insights into their mechanical performance. By doing so, the findings could contribute to refining and substantiating the arguments presented in this paper. This approach would involve assessing how various wood species, when integrated into the same truss structure, impact the structural and mechanical properties, thus allowing for a more nuanced understanding of the applicability of different wood types in the proposed structural system.



#### 4.3.3. Complexity in Real-World Construction Projects

The actual construction and implementation of the structural system in practical projects present a significant aspect that this study has not comprehensively considered. One key aspect is the assembly of structural unit nodes. In our experiments, we employed a simple model where multiple rivets were vertically inserted into the wooden members and steel cables. However, the impact of this assembly method on the structural properties of the wood and the strength of the nodes requires further validation. To address this, we propose conducting dedicated experiments on the actual construction of nodes, applying different wood joint methods to various scenarios of the new timber structure. Post-construction, various tests can be conducted to assess the actual performance, determining the influence of nodes on the entire structural unit.

Another potential challenge lies in the assembly method between structural units. Whether additional enclosure structures are needed and the specific techniques and principles for the actual assembly between structural units are crucial considerations. These factors can significantly affect the overall economic efficiency of the structure, warranting further research for substantiation.

Upon completing the proposed practical experiments, a comparative analysis can be conducted between the overall economic indicators and the related studies mentioned in the introduction (Section 1.1). This will help determine whether this new timber structural system is genuinely advanced and practically feasible on a broader scale. It is important to note that the current comparative analysis is based solely on theoretical simulated results.

#### 4.3.4. Complexity in Building Integration

Finally, the seamless integration of this new timber structural system into the broader context of building construction and its collaboration with other aspects of architecture need further validation. There are several critical considerations:

**Fire Safety:** Timber structures are prone to fire hazards. Besides treating the wood itself with fire retardants, the entire building structure must meet specified fire resistance requirements to ensure that minor fire incidents do not compromise the stability of the entire structure. Additionally, ensuring the safe evacuation of occupants in the event of a fire is a crucial aspect that requires further scrutiny.

**Compatibility with HVAC Systems:** The compatibility of this structural form with Heating, Ventilation, and Air Conditioning (HVAC) systems needs investigation. Can this structure serve as a support carrier for ventilation ducts, and is it compatible with utility rooms for plumbing, electrical, and data systems? These questions demand analysis and validation in subsequent experiments. These issues necessitate further experimental analysis and validation to ensure that the new timber structural system not only performs its role in the building structure effectively but also integrates seamlessly with other critical aspects of building design and functionality.

#### 4.4. Future Research Directions

- (1) **Study on the Applicability of Different Wood Types:** We propose further research specifically focused on exploring the suitability of various wood materials for this novel timber structural form. By utilizing different types of wood for the same truss structure, we can conduct simulations and experiments to investigate the mechanical performance. The results obtained will contribute to the refinement and validation of the viewpoints presented in this paper. The varying degrees of anisotropy in different wood types significantly affect the efficiency of wooden members in the overall structural system. These aspects require the construction of actual structural models for comparative analysis.
- (2) **Study on Different Node Assembly Methods:** After selecting suitable wood as the core compressive component for our novel timber structure, it is essential to explore different node forms. The algorithmic simulation does not currently consider the connection methods between different members, and the efficiency of load transfer

at nodes is calculated assuming 100% rigidity. Therefore, practical construction is needed to compare and select the most suitable node methods. These nodes not only need to provide sufficient structural rigidity but also require strong adaptability to meet the diverse node forms in the novel truss structure.

## 5. Conclusions

This paper addresses the challenge posed by the anisotropic nature of timber in structural design, where single timber structures struggle to accommodate multiple loads. Traditionally, this issue has been addressed by increasing material costs to enhance timber strength. The goal of this research was to design a novel structural form that allows timber to efficiently overcome this problem. Building upon the analysis of the force distribution in reinforced concrete structures, we have developed a steel–timber hybrid truss structure that optimizes the minimal load path STM through materialization, using timber for compression members and steel for tension members.

Through a thorough analysis of the experimental results, the following conclusions have been drawn. Influence of External Balance Environment on STM Morphology: By manipulating external balance environment information and adjusting the initial contour lines, we successfully generated various forms of optimized STMs. Analyzing the average load and the degree of dispersion in surplus loads of these models helped discern their structural characteristics. This indicates the capability to determine different types of optimized STMs by controlling external demands. Economic Advantages of Converting to Steel–Wood Hybrid Truss Structures: The transformation of optimized STM models into steel–wood hybrid truss structures and the subsequent analysis of their structural material consumption demonstrate the potential for enhancing the overall economic efficiency of this novel truss system in diverse architectural scenarios. In small to medium-scale buildings, a material consumption saving of 15–20% is achievable, while in medium to high-scale buildings, savings of 5–10% can be realized. This outcome underscores the potential of the new timber structural system to reduce overall structural costs. In summary, the experimental analysis provides insights into the impact of controlling external balance environment on STM morphology and the economic advantages of the new steel–wood hybrid truss system in various architectural contexts. These findings offer robust support and guidance for further applications and research in the field of novel timber structures.

However, this approach has its shortcomings and areas for improvement. The primary limitation of this topological optimization algorithm is its constraint to planar calculations. Consequently, in practical applications, it can only be deployed as a specialized shear wall. Combining these optimal solutions in the most suitable manner is thus severely restricted. In contrast, Polyframe appears more effective in simulating the generation of three-dimensional fully compressed truss structures, producing intricate forms such as shells and funnel structures [41,42]. However, when dealing with cantilever or complex hybrid structures, a more robust optimization algorithm is necessary. We identify two main directions for future optimization. Transition to Three-Dimensional Truss Optimization: Expanding the optimization algorithm from two-dimensional plane optimization to three-dimensional truss optimization is crucial. This requires the algorithm to cover the calculation of loads transmitted through three-dimensional space. Integration with Machine Learning: Combining the algorithm with machine learning is another promising avenue. Quantifying the impact of different external balance environments on the final optimized STM and attempting to empower machines with experiential judgment can lead to automatically modifying external balance environments and generating ‘load-optimized paths.’ This integration with machine learning holds the potential to enhance the adaptability and efficiency of the optimization process.

**Author Contributions:** Conceptualization, Y.G., Y.S. and M.A.; methodology, Y.G., Y.S. and M.A.; software, Y.G., Y.S. and M.A.; validation, Y.G. and Y.S.; formal analysis, Y.G.; investigation, Y.G. and Y.S.; resources, Y.G.; data curation, Y.G.; writing—original draft preparation, Y.G.; writing—review

and editing, Y.S. and M.A.; visualization, Y.S. All authors have read and agreed to the published version of the manuscript.

**Funding:** The funding resources for the development of the course and developing the research on this topic were provided by the Weitzman School of Design, University of Pennsylvania, and also the National Science Foundation CAREER Award (NSF CAREER-CMMI 1944691) to Masoud Akbarzadeh.

**Data Availability Statement:** Data are contained within the article.

**Acknowledgments:** The content of this research was produced in an advanced design research studio (ARCH-705) as part of the Master of Science in Advanced Architectural Design course taught by Masoud Akbarzadeh at the Weitzman School of Design. Yao Lu supported the computational development of this research as his teaching assistant for this course. Salma Mozaffari produced the foundational software for this work as part of her Ph.D. research on the topic of strut-and-tie methods for concrete.

**Conflicts of Interest:** The authors declare no conflict of interest.

## References

1. *EN 1995-1-1*; Eurocode 5: Design of Timber Structures-Part 1-1: General-Common Rules and Rules for Buildings. CEN: Brussels, Belgium, 2004.
2. Bello-Bravo, J.; Lutomia, A.N. Sustainable development or developmental sustainability: Two cases of indigenous knowledge and practices for sustainable sourcing for wood-based design-solutions. *Trees For. People* **2022**, *8*, 100253. [[CrossRef](#)]
3. Silva Bertolini, M.; de Moraes, C.A.G.; Christoforo, A.L.; Bertoli, S.R.; dos Santos, W.N.; Lahr, F.A.R. Acoustic absorption and thermal insulation of wood panels: Influence of porosity. *Bioresources* **2019**, *14*, 3746–3757. [[CrossRef](#)]
4. Švajlenka, J.; Pošiváková, T. Innovation potential of wood constructions in the context of sustainability and efficiency of the construction industry. *J. Clean. Prod.* **2023**, *411*, 137209. [[CrossRef](#)]
5. Dalalah, D.; Khan, S.A.; Al-Ashram, Y.; Albeetar, S.; Abou Ali, Y.; Alkhouli, E. An integrated framework for the assessment of environmental sustainability in wood supply chains. *Environ. Technol. Innov.* **2022**, *27*, 102429. [[CrossRef](#)]
6. Zubizarreta, M.; Cuadrado, J.; Orbe, A.; García, H. Modeling the environmental sustainability of timber structures: A case study. *Environ. Impact Assess. Rev.* **2019**, *78*, 106286. [[CrossRef](#)]
7. Radwan, M.; Albadri, N.M.; Thiel, D.V.; Espinosa, H.G. Near-field measurements for wood anisotropy using cavity-backed slot antennas. *NDT E Int.* **2023**, *137*, 102854. [[CrossRef](#)]
8. Perlin, L.P.; de Andrade Pinto, R.C.; do Valle, Â. Ultrasonic tomography in wood with anisotropy consideration. *Constr. Build. Mater.* **2019**, *229*, 116958. [[CrossRef](#)]
9. Marmier, A.; Miller, W.; Evans, K.E. Negative Poisson's ratio: A ubiquitous feature of wood. *Mater. Today Commun.* **2023**, *35*, 105810. [[CrossRef](#)]
10. Arcuri, D.; Magatelli, S.; Martinelli, P. Application of the tying force method in the design of alternative load paths in post-and-beam timber structures: A case building. *J. Build. Eng.* **2023**, *78*, 107577. [[CrossRef](#)]
11. Müller, K.; Grönquist, P.; Cao, A.S.; Frangi, A. Self-camber of timber beams by swelling hardwood inlays for timber-concrete composite elements. *Constr. Build. Mater.* **2021**, *308*, 125024. [[CrossRef](#)]
12. Giongo, I.; Schiro, G.; Riccadonna, D. Innovative pre-stressing and cambering of timber-to-timber composite beams. *Compos. Struct.* **2019**, *226*, 111195. [[CrossRef](#)]
13. Geno, J.; Goosse, J.; Van Nimwegen, S.; Latteur, P. Parametric design and robotic fabrication of whole timber reciprocal structures. *Autom. Constr.* **2022**, *138*, 104198. [[CrossRef](#)]
14. Koch, S.M.; Grönquist, P.; Monney, C.; Burgert, I.; Frangi, A. Densified delignified wood as bio-based fiber reinforcement for stiffness increase of timber structures. *Compos. Part A Appl. Sci. Manuf.* **2022**, *163*, 107220. [[CrossRef](#)]
15. Rankine, W.M. Principle of the equilibrium of polyhedral frames. *Lond. Edinb. Dublin Philos. Mag. J. Sci.* **1864**, *27*, 180. [[CrossRef](#)]
16. Maxwell, J.C. XLV. On reciprocal figures and diagrams of forces. *Lond. Edinb. Dublin Philos. Mag. J. Sci.* **1864**, *27*, 250–261. [[CrossRef](#)]
17. Van Mele, T.; Lachauer, L.; Rippmann, M.; Block, P. Geometry-based understanding of structures. *J. Int. Assoc. Shell Spat. Struct.* **2012**, *53*, 285–295.
18. Mazurek, A.; Carrion, J.; Beghini, A.; Baker, W.F. Minimum weight single span bridge obtained using graphic statics. In *Proceedings of the IASS Annual Symposia, IASS 2015 Amsterdam Symposium: Future Visions—Graphic Computation, Amsterdam, The Netherlands, 17–20 August 2015*; International Association for Shell and Spatial Structures (IASS): Madrid, Spain, 2015; pp. 1–12.
19. Wang, S.; Bertagna, F.; Ohlbrock, P.O.; Tanadini, D. The Canopy: A Lightweight Spatial Installation Informed by Graphic Statics. *Buildings* **2022**, *12*, 1009. [[CrossRef](#)]
20. Schlaich, J.; Schafer, K. Design and detailing of structural concrete using strut-and-tie models. *Struct. Eng.* **1991**, *69*, 113–125.
21. Xia, Y.; Langelaar, M.; Hendriks, M.A. Automated optimization-based generation and quantitative evaluation of Strut-and-Tie models. *Comput. Struct.* **2020**, *238*, 106297. [[CrossRef](#)]

22. Xia, Y.; Langelaar, M.; Hendriks, M.A. Optimization-based three-dimensional strut-and-tie model generation for reinforced concrete. *Comput. Aided Civ. Infrastruct. Eng.* **2021**, *36*, 526–543. [[CrossRef](#)]
23. Abdul-Razzaq, K.S.; Dawood, A.A. Corbel strut and tie modeling—Experimental verification. *Structures* **2020**, *26*, 327–339. [[CrossRef](#)]
24. Mozaffari, S.; Akbarzadeh, M.; Vogel, T. Graphic statics in a continuum: Strut-and-tie models for reinforced concrete. *Comput. Struct.* **2020**, *240*, 106335. [[CrossRef](#)]
25. Zhou, E.L.; Wu, Y.; Lin, X.Y.; Li, Q.Q.; Xiang, Y. A normalization strategy for BESO-based structural optimization and its application to frequency response suppression. *Acta Mech.* **2021**, *232*, 1307–1327. [[CrossRef](#)]
26. Amir, O.; Sigmund, O. Reinforcement layout design for concrete structures based on continuum damage and truss topology optimization. *Struct. Multidiscip. Optim.* **2013**, *47*, 157–174. [[CrossRef](#)]
27. Van Mele, T.; Block, P. Algebraic graph statics. *Comput. Aided Des.* **2014**, *53*, 104–116. [[CrossRef](#)]
28. Shi, X.; Park, P.; Rew, Y.; Huang, K.; Sim, C. Constitutive behaviors of steel fiber reinforced concrete under uniaxial compression and tension. *Constr. Build. Mater.* **2020**, *233*, 117316. [[CrossRef](#)]
29. *BS EN1991-1-4:2005*; Eurocode 1: Actions on structures—Part 1-4: General actions—Wind actions. British Standard: London, UK, 2006.
30. Porteous, J.; Kermani, A. *Structural Timber Design to Eurocode 5*; John Wiley & Sons: Hoboken, NJ, USA, 2013.
31. Younis, A.; Dodoo, A. Cross-laminated timber for building construction: A life-cycle-assessment overview. *J. Build. Eng.* **2022**, *52*, 104482. [[CrossRef](#)]
32. Zheng, H.; Guo, Z.; Liang, Y. Iterative Pattern Design via Decodes Python Scripts in Grasshopper. In Proceedings of the 18th CAAD Futures Conference, Daejeon, Republic of Korea, 26–28 June 2019.
33. Santner, T.J.; Duffy, D.E. *The Statistical Analysis of Discrete Data*; Springer Science & Business Media: Berlin/Heidelberg, Germany, 2012.
34. Hirji, K.F. *Exact Analysis of Discrete Data*; CRC Press: Boca Raton, FL, USA, 2005.
35. Altman, D.G.; Bland, J.M. Standard deviations and standard errors. *BMJ* **2005**, *331*, 903. [[CrossRef](#)]
36. Leys, C.; Ley, C.; Klein, O.; Bernard, P.; Licata, L. Detecting outliers: Do not use standard deviation around the mean, use absolute deviation around the median. *J. Exp. Soc. Psychol.* **2013**, *49*, 764–766. [[CrossRef](#)]
37. Ahmad, S.; Lin, Z.; Abbasi, S.A.; Riaz, M. On efficient monitoring of process dispersion using interquartile range. *Open J. Appl. Sci.* **2012**, *2*, 39–43. [[CrossRef](#)]
38. Wan, X.; Wang, W.; Liu, J.; Tong, T. Estimating the sample mean and standard deviation from the sample size, median, range and/or interquartile range. *BMC Med. Res. Methodol.* **2014**, *14*, 135. [[CrossRef](#)] [[PubMed](#)]
39. Larsson, C.; Abdeljaber, O.; Bolmsvik, Å.; Dorn, M. Long-term analysis of the environmental effects on the global dynamic properties of a hybrid timber-concrete building. *Eng. Struct.* **2022**, *268*, 114726. [[CrossRef](#)]
40. Jockwer, R.; Grönquist, P.; Frangi, A. Long-term deformation behaviour of timber columns: Monitoring of a tall timber building in Switzerland. *Eng. Struct.* **2021**, *234*, 111855. [[CrossRef](#)]
41. Nejur, A.; Akbarzadeh, M. Polyframe, efficient computation for 3d graphic statics. *Comput. Aided Des.* **2021**, *134*, 103003. [[CrossRef](#)]
42. Sinthong, P.; Carey, M.J. PolyFrame: A retargetable query-based approach to scaling dataframes. *Proc. VLDB Endow.* **2021**, *14*, 2296–2304. [[CrossRef](#)]

**Disclaimer/Publisher’s Note:** The statements, opinions and data contained in all publications are solely those of the individual author(s) and contributor(s) and not of MDPI and/or the editor(s). MDPI and/or the editor(s) disclaim responsibility for any injury to people or property resulting from any ideas, methods, instructions or products referred to in the content.